J. Fluid Mech. (1969), *vol.* 38, *part* 4, *pp.* 679–688
Printed in Great Britain

Disintegration of charged liquid jets

By A. L. HUEBNER

Rocketdyne, a Division of North American Rockwell Corporation,
Canoga Park, California

(Received 14 October 1968)

Disintegration processes occurring with charged liquid jets of distilled water have been examined. High-speed photographic techniques were used to determine the effect of charging on disintegration of the jet, the size distribution of the drops formed, and the velocities of the drops. At relatively small currents, the jet remains undisplaced while the drops formed acquire components of velocity perpendicular to the jet axis. At sufficiently large currents, the jet develops kink or longitudinal instabilities which can cause the jet to be appreciably displaced, and the drops may have relatively large components of velocity perpendicular to the jet axis. The size distributions of the drops formed are significantly different from those resulting in the absence of electrification. Mean drop size decreases with increased charging in all cases. Drop speeds increase with increased charging as a result of both increased electrical repulsion and reduction in size.

Introduction

Liquid jet disintegration and the dynamics of the droplets formed have been the subjects of intensive study since the second half of the last century. Rayleigh (1878, 1892) examined the instability of cylindrical jets and their breakup under the action of surface tension. His analysis led to the well-known result:

$$\lambda = 4{\cdot}508 \times 2a, \tag{1}$$

that gives the ratio of disturbance wavelength to jet diameter for the kind of disturbance which leads most rapidly to disintegration.

Rayleigh (1882) also examined the criteria for instability of a charged cylindrical column and a charged drop. Considering the potential energy associated with electrical charge and with cohesion due to surface tension, he showed that the critical stability condition relating charge on a spherical drop, q, drop radius, a, and liquid surface tension, T, is

$$T = \frac{q^2}{16\pi a^3}. \tag{2}$$

An analogous procedure applied to a cylindrical jet of radius r carrying charge per unit length τ yielded the instability condition

$$T = \frac{2\tau^2}{3\pi a}. \tag{3}$$

Basset (1894) analyzed the stability of a liquid jet from a more comprehensive point of view, including the effects of velocity, viscosity and ambient fluid.

Equation (2), applicable to spherical drops, has been verified experimentally under a variety of conditions. Very little experimental work has been accomplished with charged cylindrical jets. Magarvey & Outhouse (1962) investigated the breakup of water jets under combined electrical, molecular and gravitational forces. As charging of the liquid was initiated, the jet was first affected at the region at which drops break off and the drops acquired small components of velocity perpendicular to the jet axis. With increased charging, rather violent 'whipping' of the jet was observed, with the formation of the jet into looping filaments. Because of the lateral displacements developed, the drops formed after severing of the filaments have substantial components of velocity perpendicular to the original jet axis. Their size distribution was observed to be altered, as well.

The present study constitutes an extension of the work reported by Magarvey & Outhouse and a quantification of observed results. High-speed photographic techniques were employed in examining electrified cylindrical distilled-water jets of several radii. The water could be treated as a conductor for all jets employed because its relaxation time of approximately 10^{-6} sec was several orders of magnitude smaller then the jet breakup time. Drop-size distributions have been determined for these jets, for varying degrees of electrification. Distributions of drop velocities were also determined. Similar effort is currently underway with other liquids to effect variation in fluid dynamic and electrical properties. This effort will be reported at a later date.

Experimental apparatus and technique

The apparatus used to produce charged liquid jets is shown schematically in figure 1. The liquid, contained in an insulating reservoir, is in contact with one terminal of a conventional high-voltage source. The other terminal is connected to ground, with ammeters located in both connexions. A grounded metal vessel collects the effluent liquid and provides the ground, or return, electrode. This collector had to be at least 4 in. in diameter because when the jet is electrified the smaller drops can move away from the jet axis at quite large angles. For a collector diameter less than 4 in., loss of droplets due to spraying over the top of the collector has been observed, even with the top located very close to the orifice. Two narrow slots are cut into the sides of the collector directly opposite each other, allowing visual and photographic observation of the jet breakup and droplet dynamics. The power supply is a conventional full-wave doubler with a maximum rating of 50 kV at 20 mA. All tests were conducted with a potential difference between jet and collector of 25 kV or less to limit corona effects to negligible levels.

Still photography, utilizing a 4 by 5 Speed Graphic or a Polaroid camera, was employed to establish the sizes of the jet diameter for various orifice diameters and velocities of efflux, and to adjust backlighting so that the liquid jet, the disintegration region, and the droplets formed would all be clearly recorded

on the motion-picture photographic record for subsequent reduction and analysis. High-speed motion picture photography was accomplished utilizing a modified Wollensak Fastax camera. The framing mechanism was removed from the camera and a magnetic pickup coil was installed near the drive sprocket. Framing

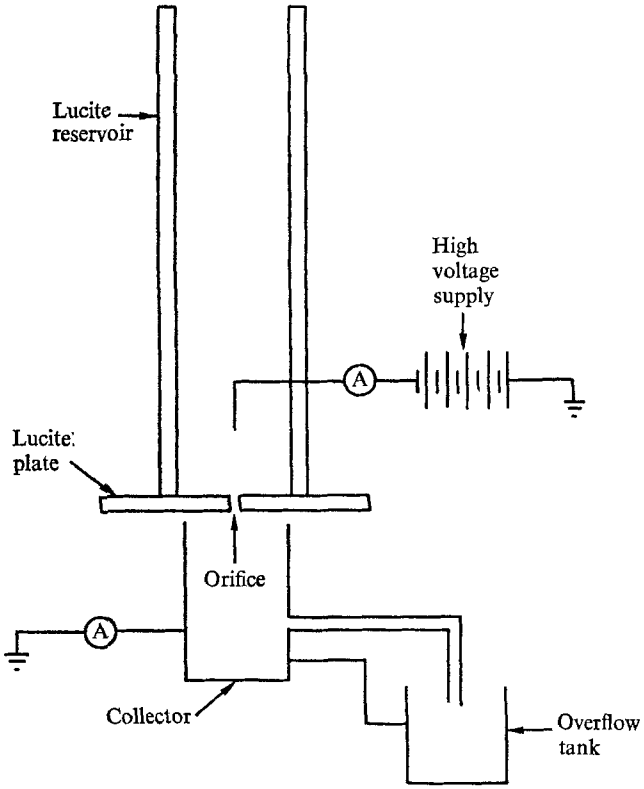

FIGURE 1. Schematic diagram of electrification apparatus.

is achieved by using the magnetic pickup coil as a trigger. Each time one of the drive sprocket pins passes the pickup coil, a pulse is delivered to the strobe trigger circuit that fires the flashlamp. This method ensures synchronization of camera and strobe at all film speeds. A short-duration (approximately 1 μsec) light pulse was used to effectively 'freeze' all motion. Timing marks were recorded on the film so that the time increment between frames could be determined accurately for the purpose of establishing droplet velocities.

Disintegration of jets

Variation of the disintegration of a charged distilled water jet under one set of flow conditions is shown in figure 2, plate 1. The uncharged jet is depicted in figure 2 (*a*), with typical jet disintegration and drop formation exhibited. The pattern of jet disintegration and droplet formation that occurs at a quite low electrification is shown in figure 2 (*b*). The disturbance introduced by the presence

of charge on the jet is apparent for a distance of several diameters above the point of drop formation, but is most pronounced at that point. This activity in the drop formation region causes the drops to acquire components of velocity perpendicular to the vertical. The formation of smaller drops than those exhibited in the uncharged case is also apparent. At somewhat higher electrification (figure 2 (*c*)) the current carried by the jet is sufficient, for the flow conditions indicated, to cause the pronounced distension of the jet, and the displacements of the distended portions from the original jet axis, which is characteristic of the longitudinal instability described by Wuerker *et al.* (1967). The 'whipping' motion is quite violent, as seen in motion picture sequence. The violence of the activity is also implied by the drop distribution and loss of focus in figure 2 (*c*).

A similar sequence of photographs for the same size jet but with increased flow-rate is shown in figure 3, plate 2. The jet breaks up in a shorter time when it carries a small current (figure 3 (*b*)) than with no current, but only the usual 'sausage' instability is observed in both cases. The mode of jet instability changes with increased electrification, but, at jet currents up to those consistent with maintaining negligible corona loss, longitudinal instability of the jet does not occur (figure 3 (*c*)). It is probable, however, that the longitudinal instability would occur at currents higher than 20 μA.

The combined kink and sausage instability shown in figure 3 (*c*) is of special interest because its occurrence has not been reported by previous investigators. Magarvey & Outhouse pay considerable attention to the formation of drops from a whipping jet, with the largest drops being formed near the jet axis and the smallest drops formed at the greatest lateral displacement. It is clear that at the intermediate conditions corresponding to those shown in figure 3 a completely different drop-formation pattern is attained. The manner in which drop formation occurs also pronouncedly influences the distribution of drop velocities, as will be shown.

The pattern of disintegration with the largest jet used is indicated in figure 4, plate 3. This case differs from the preceding in that the flow of the jet is turbulent. The sausage instability that develops in the lower region of the uncharged jet appears to be quite ragged, but reasonable drop formation is obtained well below the discharge orifice. A small jet current (figure 4 (*b*)) promotes the instability, causing drop formation nearer to the discharge orifice. However, some of the elements formed represent substantial pieces of the jet and develop sausage instability, in turn forming drops. The small drops appearing in figure 4 (*b*) and (*c*) are noteworthy. The satellite droplets which form from the uncharged jet do not persist, but instead quickly coalesce with the larger drops. The current carried by the jet of figure 4 (*b*), (*c*), in addition to decreasing the size of the principal drops formed, causes the satellites to move laterally from the jet axis so that coalescence is avoided and the smallest drops are preserved in the distribution.

Figure 4 (*c*) shows the effect produced with the largest current employed during the course of the study. The current is sufficient, even with this relatively large jet and flow-rate, to produce the combined kink and sausage instabilities observed previously. The incipient drops at the lower end of the unbroken jet are dis-

torted by the presence of charge. At this jet current, the distortion is great enough to form pointed regions on the drops from which fine filaments of liquid are ejected, as in figure 4(*d*).

Drop-size distributions

Direct measurement of drop images on motion-picture photographic records of disintegrating jets was employed to quantify the indicated decrease in the sizes of drops formed from electrified jets. Diameter measurements on approximately 400 drops were needed to obtain a statistically meaningful, reproducible sample. After sorting by size, the number of drops in each size interval was divided by the magnitude of the interval. This distribution was then plotted in smoothed form, after normalizing to a total of 1000 drops so that direct comparison of various distributions was possible.

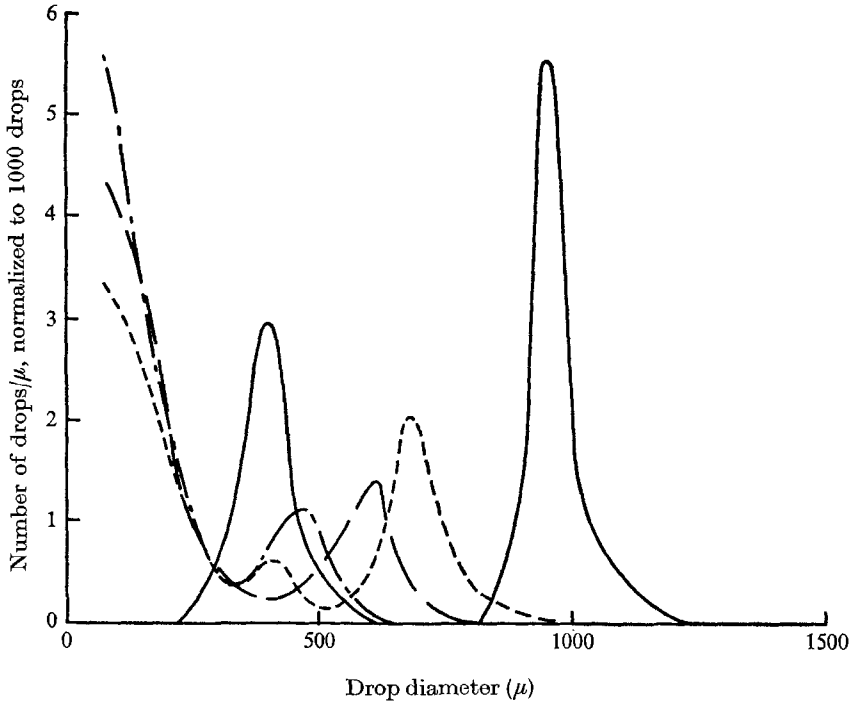

FIGURE 5. Drop size distribution for various currents: ——, 0 μA; - - - -, 5 μA; – – –, 10 μA; — . —, 15 μA. Jet diameter, 0·493 mm; flow-rate, 0·49 ml/sec.

Typical drop-size distributions are shown in figures 5 and 6. The uncharged water jet of diameter 0·493 mm forms drops of two different sizes. The largest number is formed with a diameter slightly less than 1000 μ, in good agreement with the expression

$$d = 1{\cdot}89D, \tag{4}$$

where d is the drop diameter and D the jet diameter. Equation (4) follows from (1) under the idealized condition of equating the volume of a spherical drop to

the volume of a cylinder of fluid of diameter D and length λ. The peak at this drop size is quite free from scatter, while a secondary peak, occurring at a diameter slightly less than the jet diameter, exhibits somewhat greater scatter. When the jet is electrified, the largest-diameter drops formed become considerably smaller and considerably less numerous than for the uncharged jet, and a

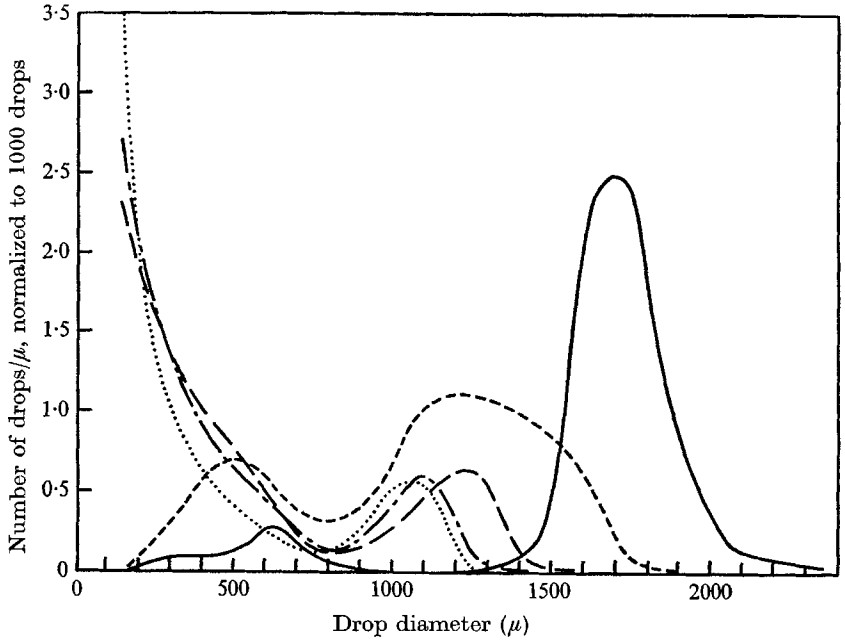

FIGURE 6. Drop size distribution for various currents: ——, 0 μA; – – –, 2 μA; ——, 5 μA; – – -, 10 μA; - - - -, 15 μA. Jet diameter, 0·80 mm; flow-rate, 0·43 ml/sec.

large number of very small drops are formed. This trend continues with increasing electrification until, at the highest current, the largest drops are only approximately one-half the diameter of the largest drops formed from the uncharged jet and the number of small drops formed is very pronounced. (Drop diameters smaller than approximately 70 μ are too small to be resolved by the optical system used to reduce the photographic data, accounting for the form of the curves at very small diameters.)

A plot of drop-size distributions for a larger jet is shown in figure 6. The same general features of drop size alteration with increasing jet current occur as in the preceding case. Interestingly, while the initial small electrification of the jet (2 μA) causes a decrease in both primary peak diameter and relative frequency of formation, a slightly greater electrification (5 μA) further reduces the frequency but does not affect the diameter appreciably. The trend toward increased formation of small drops with increased electrification is preserved and any of the mean diameter quantities conventionally used to characterize drop size distributions will exhibit a lowering of mean diameter with increasing jet current.

Drop velocities

It is apparent from the photographs that droplets formed from the disintegration of electrified jets move with components of velocity perpendicular to the axis of the undisturbed jet. Magarvey & Outhouse reported that drops were observed leaving the formation point at high velocities in directions making a relatively large angle with the vertical. This observation was for drop sizes smaller (5 to 25 μ) than those considered here. Explicit details of the flow and electrical conditions under which these results were observed were not given. Other literature on the subject is equally limited concerning droplet velocities, although a knowledge of the direction of droplet velocities is vitally important in applications. Consequently, motion picture records were examined to determine velocities associated with drops formed from electrified jets.

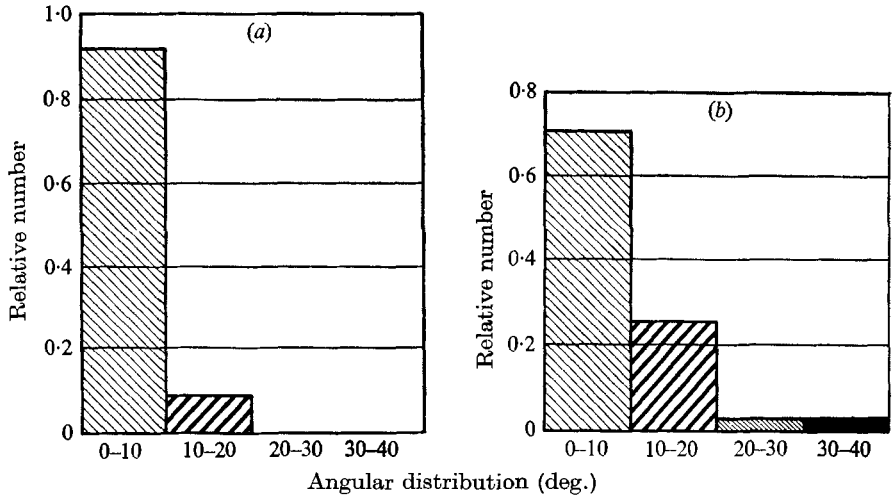

FIGURE 7. Angular distribution of drop velocities at two different currents. (*a*) I = 5 μA; D = 750 μ (nominal). (*b*) I = 10 μA; D = 610 μ (nominal).

Figure 7 shows results that typify the relationship among largest drop size, jet current and angle between drop velocity vector and jet axis. The results presented are for the test condition to which the drop size distribution of figure 5 corresponds. Comparison is made beween different drop sizes as current is varied because the sizes that are prominent in each distribution depend upon jet current. While less than 10 % of the largest drop velocity vectors make angles greater than 10° at a current of 5 μA, this increases to nearly 30 % at a jet current of 10 μA. Furthermore, at 10 μA a small percentage of the drops are in an angular range as high as 30–40°.

The variation in angular distribution for smaller drops is indicated in figure 8. The results are different from what might be anticipated. Drops of nominally 200 μ diameter move at relatively large angles at a jet current of 5 μA, as might be expected. However, the distribution is toward lower angles when current is increased to 10 μA. Although these results are surprising, an explanation can be made upon examining the patterns of jet disintegration and droplet formation

which occur at the two current levels being compared. The instability created at 5 μA is such as to promote sausage instability, with only a very slight kink instability. Consequently, near the point of formation, the drops are not very far from the vertical jet axis. The small drops are then able to move away from the point of formation at relatively large angles with respect to the direction of the undisturbed jet. The larger charge on the larger drops does not tend to impede large-angle motion.

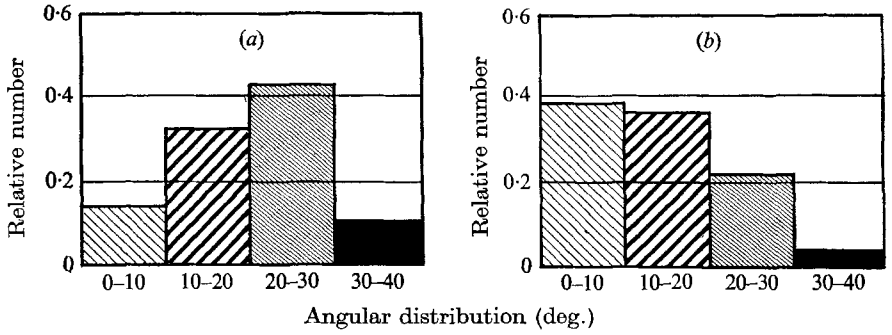

FIGURE 8. Angular distribution of drop velocities at two different currents. (*a*) I = 5 μA; D = 200 μ (nominal). (*b*) I = 10 μA; D = 200 μ (nominal).

Current (μA)	Drop size (nominal, μ)	Average speed (mm/sec)
0	950	3100
5	200	5400
5	750	4230
10	200	6070
10	610	5000

TABLE 1. Average speed for various drop sizes.

When the jet current is increased to 10 μA the kink instability is enhanced (somewhat as in figure 3 (*c*)). The larger drops are then formed at relatively large displacements from the jet axis, while the small drops develop from the filaments connecting the large drops. To some extent then, the charged large drops form a barrier against lateral motion of the similarly charged small drops, reducing their tendency to move from the jet axis at large angles. This general picture of drop motion is confirmed by frame-by-frame analysis of the motion-picture sequences.

The charge on the jet influences the magnitudes of drop velocities (speeds) as well as introducing changes in the angular distribution. The test conditions just considered were examined further to establish the effect of jet current on the average speed of droplets, using the same basis of comparison as was used in considering the angular distribution. The average speed for each of the drop sizes was computed, and the results are listed in table 1. Mean speeds of the chief drop size components formed from the uncharged jet are included for comparison.

Discussion

The experiments described in previous sections exhibit patterns of electrified jet disintegration which are, in many respects, as anticipated and as reported by previous investigators. However, combinations of instabilities not previously reported (notably combined kink and sausage modes) were observed for a variety of flow and electrical conditions. These combinations are significant in that they lead to droplet distributions which contrast in two important ways with those discussed by Magarvey & Outhouse for jets breaking up under longitudinal instabilities. First, the distance from the jet axis of large and small drop formation is reversed. Our own experiments on jets disintegrating in the longitudinal mode confirm observations that the smaller drops are formed at the regions of greatest displacement from the axis, with the larger drops forming near the axis. But the opposite is true for a jet breaking up in the combined mode, and the combined mode of breakup can occur over a broad range of flow and electrification conditions. Secondly, in the longitudinal mode of breakup, the smaller drops always move off at larger angles with respect to the jet axis than the larger drops. In combined mode, however, a more complex pattern of velocity distribution occurs, which depends, essentially, on the relative development of the kink instability.

The experiments confirm the formation of smaller drops from a disintegrating jet as the jet is electrified, as reported by Magarvey & Outhouse. More importantly the techniques employed provide data for the quantification of this decrease in size. Quantification in turn shows any of the mean diameters conventionally employed in considering drop size distribution to be a monotonically decreasing function of jet current. This suggests the possibility of employing electrification to effect a considerable amount of control over the technologically important problem of drop formation from liquid jets. Propellant drop size, for example, is of fundamental importance in combustion phenomena, where it is frequently desirable to obtain the smallest possible drops. The work reported here indicates that charged jets can offer a significant advantage in reducing the size of drops formed from jets.

Theoretical treatments to date of drop formation from jets offer little explanation of the observed results. Equation (4), well verified for drops formed from unelectrified jets, is developed from consideration of the wavelength of the fastest growing perturbation on the jet. Electrification of the jet influences the length of the fastest-growing wave as well as altering the overall pattern of instability. From consideration of these influences it appears possible to rederive equation (4) for electrified jets. This rederivation is currently in progress.

This research was sponsored by the Office of Naval Research under Contract N00014-67-C-0474, Contract Identification no. NR 094-358.

REFERENCES

BASSET, A. B. 1894 *Amer. J. Math.* **16**, 13.

MAGARVEY, R. H. & OUTHOUSE, L. E. 1962 *J. Fluid Mech.* **13**, 151.

RAYLEIGH, LORD 1878 *Proc. London Math. Soc.* **10**, 4.

RAYLEIGH, LORD 1882 *Phil. Mag.* **14**, 184.

RAYLEIGH, LORD 1892 *Phil. Mag.* **34**, 145.

WUERKER, R. F., HEFLINGER, L. O. & BROADWELL, J. E. 1967 *ARL* 67-0211, Office of Aerospace Research, USAF.